MR Imaging of Cerebral Hematomas at Different Field Strengths: Theory and Applications

Rodney A. Brooks, Giovanni Di Chiro, and Nicholas Patronas

Abstract: Existing theory on relaxation effects in blood and their field dependence is related to magnetic resonance (MR) imaging of hematomas. These effects include (a) relaxation caused by protein and other macromolecules; (b) inhomogeneous susceptibility created by paramagnetic forms of hemoglobin (Hb) (deoxy and met) within the red blood cells; and (c) direct interaction of water protons with paramagnetic metHb. The effect of proton density is also discussed. These effects combine in a complex way to create hypo- or hyperintensity on MR images of hematomas. Further, the effects change as the hematoma evolves both physically and chemically. In particular, there are five stages that are associated with typical image appearance: (a) oxygenated blood; (b) deoxygenated blood; (c) conversion to metHb; (d) hemolysis; and (e) protein resorption. Index Terms: Blood—Magnetic resonance imaging, techniques—Hematoma—Brain, hemorrhage.

Computed tomography produced a breakthrough in the diagnosis of intracerebral hematomas and rapidly replaced older and less specifically diagnostic imaging methods such as pneumoencephalography and angiography. The interpretation of CT images in cases of intracerebral hematomas was and remains straightforward (1–5). Fresh hematomas appear hyperdense compared to normal brain tissue because of the high mass density of hemoglobin (Hb). The hyperdensity may increase slightly as the clot retracts, but eventually, after 2–6 weeks, the appearance becomes hypodense owing to the influx of watery fluid and resorption or breakdown of protein. Magnetic resonance (MR) imaging of hematomas has been a different story. The radiologist must cope with a variety of unfamiliar tissue properties, which change as the hematoma evolves and which depend in a complex way on magnetic field.

Following is an abbreviated history of published reports on MR of intracerebral hematomas. Early reports on chronic clinical hematomas mentioned

From the Neuroimaging Section, NINCDS, National Institutes of Health, Bethesda, MD (R. A. Brooks and G. Di Chiro), and Radiology Department, Georgetown University Medical School, Washington, D.C. (N. Patronas). Address correspondence and reprint requests to Dr. R. A. Brooks at Neuroimaging Section, NINCDS, National Institutes of Health, Bethesda, MD 20892, U.S.A.

short T1 and long T2 values compared to brain parenchyma (6–10), whereas an early report of an experimental acute lesion (11) described long T1. Moon et al. (10) suggested that the appearance would change as the composition and structure of the hematoma evolved, and such a change was described by Sipponen et al. (12), who found a shortening of T1 with age of lesion at 0.17 T. In 1984 DeLaPaz et al. (13) noted a shortening of T2 due to deoxygenation, which disappears with hemolysis, and later Gomori et al. (14) emphasized the importance of field strength in this effect. In 1985 Bradley and Schmidt (15) linked early T1 shortening to the conversion of hemoglobin (Hb) to metHb. Di Chiro et al. (16) demonstrated in vivo and in vitro that T1 and T2 shortened during the first week, in correlation with the formation of metHb, and that subsequently T2 increased. In 1986 Edelman et al. (17) showed that T2 lowering due to deoxygenation can also be seen at moderate fields (0.6 T) with a gradient echo imaging technique. In the meantime, Sipponen et al. (18) reported low T1s in acute hematomas at very low field strength: 0.02 T.

Given this complexity, it is not surprising that much confusion exists, not only in the radiological, but even in the physics communities. There are conflicting views about the importance of various effects, and even about their existence. It is not our goal to take sides among the various factions, but

rather to present what is known and what has been reported on its own merit. We will emphasize the dependence of the various effects on magnetic field, because imaging strategy is quite different at different fields.

In the following discussions, for convenience, we divide imaging field strengths (and Larmor frequencies) into three ranges:

Low: 0.01–0.1 T (0.4–4 MHz)—typical of resistive air core magnets

Medium: 0.1–0.5 T (4–21 MHz)—typical of iron core magnets (including permanent)

High: 0.5–2.0 T (21–85 MHz)—typical of superconducting magnets

This categorization is arbitrary and is but an approximation to the gradual dependence on field exhibited by most effects.

THEORY

The tissue parameters relevant to hematoma imaging are nuclear magnetic relaxation times and proton density. (Flow effects, although important when imaging blood vessels, are not relevant to the imaging of stationary blood.) Nuclear relaxation refers to the reorientation (usually exponential) of nuclear spins following a disturbance. Longitudinal relaxation, described by a time constant $T1$, is the realignment of spins along the applied magnetic field, while transverse relaxation, with time constant $T2$, represents the loss of coherent transverse magnetization and hence of MR signal. $T2$ is generally shorter than $T1$ because of microscopic field variations, or other disturbances, that create phase differences among the precessing protons.

In Section I below we describe the known relaxation mechanisms that contribute to $T1$ and $T2$ of blood and hematomas. Proton density effects are discussed in Section II. A more mathematical review of this material may be found elsewhere (19).

I. Relaxation Times

The presence of Hb in blood affects relaxation times in three different ways. First, we will discuss diamagnetic effects that are present with all forms of Hb, including oxyHb, which is nonparamagnetic. These effects have not been previously emphasized in the radiological literature and so are described in some detail. Then, we cover the presence of paramagnetic forms of Hb (deoxyHb and metHb) within the red blood cells, which leads to inhomogeneous susceptibility effects. Finally, we describe direct relaxation caused by paramagnetic molecules, which is significant only with metHb. These effects are summarized in Table 1.

TABLE 1. *Three relaxation effects caused by hemoglobin (Hb) in blood*

Effect	Type of Hb	Lowers	At field strength
Protein "water of hydration"	All (enhanced if intracellular)	T1 T2	L All
Inhomogeneous susceptibility	DeoxyHb and metHb (intracellular only)	T2 T2*	H M and H
Paramagnetic relaxation	MetHb	T1 and T2	All

The indicated field ranges (L – 0.01–0.1 T, M = 0.1–0.5 T, H – 0.5–2 T) give an approximate indication of the gradual dependence of each effect on magnetic field.

A. Protein Effects (T1 and T2)

In the absence of paramagnetism, proton relaxation in water solutions is caused by the changing magnetic field of nearby nuclei, particularly the neighboring intramolecular proton, as the molecule undergoes Brownian motion (20,21). This theory was strikingly successful in explaining the observed $T1$ of pure oxygen-free water at 37°C: $T1 = 4.5$ s (22). $T2$ was found to be somewhat smaller, 2.9 s, because of the presence of ^{17}O (23).

Relaxation times are shortened in the presence of protein and other macromolecular structures because water molecules are slowed down by them. One such slowing down effect has been attributed by Koenig (24) to surface polar groups on the macromolecules. This effect alone reduces $T1$ and $T2$ in blood at 37°C to <1 s and is independent of field strength for Larmor frequencies up to 100 MHz.

In addition to "surface" relaxation, a second relaxation component is present in blood, which has a strong field dependence corresponding to the Brownian motion of protein molecules. This component is usually attributed to water of hydration, i.e., water molecules temporarily attached to proteins, although other mechanisms have been suggested (24). For notational convenience we continue to use the term "water of hydration," without attempting to arbitrate between the mechanisms. As we will see, water of hydration affects $T1$ primarily at low fields, further reducing it to about 200 ms at very low fields, in agreement with existing blood data. $T2$, on the other hand, is affected at all fields, with a predicted value of about 350 ms at high fields; however measured $T2$ data are lower still, indicating the presence of still other unknown relaxation effects.

The protein effects are clearly dependent on, and generally proportional to, protein concentration. This dependence is relevant to MR of hematomas, since the Hb concentration changes during evolution of the hematoma, becoming higher with clot retraction and lower with protein resorption. In ad-

dition, we will see that the water of hydration effect is even further enhanced at the very high Hb concentration typical of erythrocytes.

T1 (low field). Each proton precesses about the applied magnetic field at the Larmor frequency f_0 (typically 1–60 MHz for MR imaging). It follows from either classical or quantum theory that changes in orientation of the proton with respect to the applied field require a varying magnetic field with an oscillating component at the Larmor frequency. This, of course, is how "excitation" and "inversion" are accomplished in typical MR pulse sequences. Thus, longitudinal relaxation can occur only if there is an oscillating field present. In the case of water protons, the oscillating magnetic field comes from nearby particles, particularly the neighboring proton within the same molecule. Because the molecule is in a constant state of thermal agitation (Brownian motion), the field of the neighboring proton changes as the molecule rotates or tumbles (20,21).

Now we must ask, How does a randomly fluctuating field produce oscillations at the Larmor frequency? A statistical analysis of Brownian motion (20,21) shows that, on the average, the random variations can be regarded as a superposition of sinusoidal oscillations with a frequency distribution (spectrum) that has constant amplitude at low frequencies and that falls gradually to zero around a half-amplitude point called the "cutoff" frequency. In other words, the thermal energy is distributed uniformly over a frequency range and then falls to zero. As the thermal energy declines with frequency, so does the relaxation effect.

An important fact is that the cutoff frequency, or upper limit of the frequency range, is inversely proportional to the size of the rotating molecule; i.e., big molecules move more slowly than small ones. Thus, as molecular size increases, the cutoff frequency falls and the thermal energy becomes concentrated in a smaller frequency range, making more energy available at the Larmor frequency. However, if the molecule is so large that the Brownian cutoff frequency is well below the Larmor frequency, there is negligible thermal energy available for longitudinal realignment. These statements also apply to water molecules that are attached to the big molecule as water of hydration or otherwise share its motion. If these molecules exchange rapidly with bulk water, the relaxation effects will be transmitted to the entire water pool. The spectra for the three categories of water described herein are illustrated in Fig. 1.

For Hb in whole blood, the Brownian cutoff frequency is ~1 MHz (19)—well in the low field range. Therefore, the effect on T1 is limited mostly to low
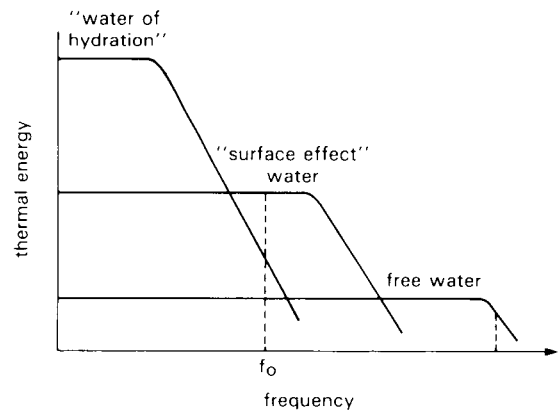

FIG. 1. Spectra of rotational Brownian motion. f_0 is typical Larmor frequency in medium field range. Lowest curve (bulk water) has high cutoff frequency, with little energy available at f_0 for T1 relaxation. Middle curve (water slowed by "surface effect") contributes more to T1 relaxation at f_0. Highest curve ("water of hydration") has low amplitude at f_0, but gives large contribution at very low Larmor frequencies.

fields, with T1 approaching ~200 ms in the low field limit. At medium and high fields, T1 approaches the value mentioned above, ~1 s.

Although the Brownian motion theory gives good agreement with T1 data for Hb solutions and for whole blood, there are some questions. Koenig (24) has suggested that the relaxation component with a cutoff frequency of 1 MHz comes from the "sloshing" of nearby bulk water, rather than from water of hydration. Zhong et al. (unpublished data) report that a significant contribution to T1 in protein solutions comes from "cross-relaxation" of water protons by protein protons. These same authors also report an exchange time for water of hydration of 23 ms, which raises further questions about the fast-exchanging water of hydration theory.

T2 (all fields). Brownian motion also contributes significantly to T2, but there is a fundamental difference: Transverse relaxation does not involve changes in energy of the proton and hence does not require an oscillating magnetic field at the Larmor frequency. Therefore, T2 is affected even for Larmor frequencies beyond the Brownian cutoff frequency. In fact, it follows from the detailed theory that the relaxation rate at high fields is 30% of the low field value (20,21). Thus, the contribution from water of hydration is significant at medium and high MR fields and, in whole blood, reduces T2 to ~350 ms.

However, the observed T2 of blood is lower still, ~200 ms at 0.5 T (16). This means that water of hydration contributes only about a third of the total relaxation rate (1/T2), with almost a third coming from free and "surface effect" water, and another third or more unaccounted for. This is in contrast with T1, which is well explained by Brownian mo-

tion theory. A possible mechanism that might account for the difference is exchange of protons between sites of slightly different Larmor frequency, i.e., chemical exchange. If the exchange is rapid compared to the relaxation rates, random phase differences occur in the population of precessing protons that are describable by a lowering of T2, without T1 being affected. Indeed, the difference between T2 and T1 in pure water was found to be due to exchange of protons to and from water molecules containing ^{17}O (23). Zhong et al. (unpublished data) have reported chemical exchange effects in protein solutions between bulk water and water of hydration involving very small chemical shifts (0.015 ppm), observable at Larmor frequencies above 100 MHz. There may be other exchange processes involving greater chemical shifts and faster exchange that would affect T2 at MR fields. This, however, is speculative, there being no published reports demonstrating the existence of such chemical exchange effects in blood.

There is one further point relevant to MR imaging of hematomas. The relaxation effect of water of hydration depends strongly on local Hb concentration (25,26), beyond the normal proportionality exhibited by all protein effects. Specifically, the high Hb concentration and tight packing within red blood cells ($\sim$5.5 mM) impede the Brownian motion, reducing the cutoff frequency to one-third of what it would be if the Hb were distributed uniformly throughout the blood. This means that the contribution to the transverse relaxation rate (1/T2) is reduced by a factor of three in hemolyzed blood, in which the Hb is spread out more dilutely. In fact, several investigators have reported higher T2 values in hemolyzed, oxygenated blood (27,28).

B. Inhomogeneous Susceptibility (T2 and T2*)

We now turn to paramagnetic effects. Even though deoxyHb is paramagnetic, its unpaired iron electron is so well sequestered that the direct interaction with free water protons is negligible. However, because the paramagnetism is confined to the red blood cells, there is an inhomogeneous distribution of susceptibility, which creates microscopic field gradients (29). In effect, each red blood cell becomes a miniature bar magnet, and water protons at different positions relative to these "magnets" experience different field strengths. The situation is similar to the chemical shift between water protons and fat protons, except that the magnitude is smaller: perhaps 0.4 ppm (30) instead of 3.5 ppm. Therefore, there is no displacement of one image relative to the other, as may occur with water and fat, but the signals superimpose on each other within a given picture element causing hypointensity.

The paramagnetic susceptibility effect is also present with intracellular metHb; in fact, metHb has a higher paramagnetic moment than deoxyHb. Further, the effect is strongest with hematocrits around 50%, dropping off at high hematocrits as the field becomes more uniform (31). This effect, of course, disappears with hemolysis, as the paramagnetism is then distributed uniformly and there is less field inhomogeneity. We also note that a similar effect has been reported when paramagnetic hemosiderin accumulates within phagocytes in later stages of hematoma evolution (14).

Inhomogeneous susceptibility affects MR imaging of hematomas two ways: First, with an ordinary spin echo sequence, signal loss occurs because of diffusion of water molecules through regions of different field (cf. effect of chemical exchange on T2 mentioned earlier). Second, with a gradient echo sequence, signal loss occurs even without diffusion. These two mechanisms are described below.

Before proceeding, a comment must be made about notation. Neither signal loss mechanism is, in general, exponential, and therefore neither is strictly describable by a time constant T2. Nevertheless, this notation is commonly used (although T2* is used with the gradient echo method, to indicate that the effect of field inhomogeneity is included). Therefore, the measured T2 may vary, depending on the echo time (TE) used to make the measurement. The problem is particularly acute with diffusion when the TE is comparable to the diffusion time through the gradients. As a reminder that nonexponential diffusion effects are included, we will use the term "effective T2."

Diffusion (T2). The effect on T2 of intracellular paramagnetic deoxyHb was reported by Thulborn et al. (31), using spin echo sequences with varying TE. The effect is due to irreversible dephasing when water molecules move between sites of different magnetic fields during the interval TE. As mentioned above, the signal loss is not exponential in time, so the T2 value so defined depends on the TE. If a series of spin echoes is observed, as with the Carr-Purcell-Meiboom-Gill technique (32), it is the interecho time that determines the effective T2, not total time to last echo. Thus, a series of echoes with short interecho time will exhibit less diffusion loss at the final echo than a single echo with the same final TE.

This signal loss, described as a reduction in effective T2, depends quadratically on field strength, and so is particularly great at high fields (31). It should be noted that there is not general agreement on whether the responsible field gradients are primarily intracellular, extracellular, or both, and what the time constant of diffusion is (27,30,31,33).

Gradient echo (T2*). Recently introduced MR

pulse sequences for fast imaging utilize a small excitation angle and "gradient echoes." For these sequences, dephasing due to field inhomogeneity is an important contributor to signal loss. Although the signal loss is not necessarily exponential (as would be the case if the inhomogeneity had a particular "Lorentzian" distribution), it is usually described by a transverse relaxation time T2*. (The "*" indicates that static field inhomogeneity effects are included.) This reduction in T2* due to intracellular paramagnetism is noticeable at medium fields and increases linearly with field strength and with deoxygenation (19,27).

C. Paramagnetic Relaxation (T1 and T2)

Direct relaxation of water protons by paramagnetic spins is a common mechanism in most paramagnetic solutions. Indeed, deoxyHb, with its sheltered paramagnetic electrons, is more of an exception than the rule. However, when deoxyHb converts to metHb, direct paramagnetic relaxation becomes effective. The Fe^{3+} ion is closer to the surface than in deoxyHb, and, in addition, the water molecule in the heme "pocket" is freer to exchange with bulk water (34). Thus, both bulk water ("outer sphere") and bound water ("inner sphere") experience paramagnetic relaxation and contribute to the observed T1 and T2. The theory is analogous to the proton-proton relaxation discussed in Section IA, although more complex. The result is a substantial reduction in both T1 and T2, which depends on metHb concentration and which is unaffected by hemolysis.

II. Proton Density

The effect of proton density on MR signal is straightforward: The more protons per unit volume, the stronger the signal, so image intensity is proportional to proton density. This is true for all imaging sequences. In the brain, the MR signal arises almost entirely from water protons, and proton density is therefore equivalent to water concentration. The water content of human whole blood has been reported as 81% (35), compared with 82 and 72% for gray and white matter, respectively (36). Thus, we would expect proton density to contribute a modest (9%) hyperintensity in fresh bleeds, as compared to white matter. As the clot retracts, we would expect the water concentration to become somewhat lower. However, much later, as protein is resorbed and the lesion becomes cyst-like, the water content increases to levels approaching 100%.

The effect of proton density has been cited by Zimmerman et al. (37) as responsible for a "mild hyperintensity" in T1-weighted images of hematomas at 12–24 h. Hackney et al. (38) reported a much stronger proton density effect in hematomas of all ages, with a calculated density 1.56 times higher than white matter (1)!

APPLICATIONS

We now attempt to correlate the above mechanisms with the appearance of hematomas on MR. The effect of relaxation times on signal intensity is complex and depends on the pulse sequence used. A short T2 always reduces signal strength, causing hypointensity, but the degree depends on the TE. On the other hand, a short T1 leads to hyperintensity with most pulse sequences, by enabling a more complete recovery of magnetization between pulse repetitions. These effects are described in more detail for four commonly used sequences in Section I below. In Section II, we describe the evolution of hematomas and relate the earlier theory to MR appearance at different magnetic fields.

I. Imaging Sequences

A. T1-Weighted Image

T1-weighted pulse sequences use short repetition time (TR) and short TE, e.g., TR 600 ms and TE 30 ms. The general requirement for optimal T1 related contrast is that TR should be approximately equal to T1 of normal tissue; TE should be kept small to minimize T2 sensitivity. Note that image intensity is inversely correlated with T1 because, since the time for realignment is limited, the tissue with the fastest realignment rate (short T1) will produce the largest signals. Also note that T2 sensitivity is merely reduced in these sequences, not eliminated, and that proton density effects are present as well.

B. T2-Weighted Image

T2-weighted pulse sequences use long TR and long TE, e.g., TR 2,500 ms and TE 100 ms. The general requirement is that TR should be long compared to tissue T1, to minimize T1 sensitivity, and TE should be comparable to the expected T2 values. In this case, image intensity is directly correlated with T2, since short T2 means loss of signal and hence hypointense images. If TR is sufficiently long (four times T1 is recommended), T1 sensitivity is virtually eliminated, although proton density still affects the image intensity proportionally.

C. Short Inversion Recovery (STIR)

Inversion recovery sequences begin with a 180° pulse that inverts the longitudinal magnetization

with respect to the static field. While realignment is occurring (with time constant T1), a 90° excitation pulse is applied at an inversion time (TI) later and the spin echo is observed. If TI is <70% of the shortest T1 of the tissue being imaged, changes in both T1 and T2 will contribute synergistically to contrast in the absolute magnitude image. This occurs because the echo is observed while the magnetization is still antiparallel to the field and decreasing in absolute magnitude. Tissues with shorter T1s produce less absolute signal because the longitudinal magnetization is closer to zero at the echo, just as shorter T2s lead to less signal because of rapid dephasing of the echo. A second synergism involves T1 and proton density, with increases in both working together to give hyperintensity on the image. The sequence has been called STIR, for Short TI Inversion Recovery (39).

D. Gradient Echo Image

Gradient echo imaging was introduced into MR as a necessary ingredient of fast imaging, along with short TRs and small flip angles (40). It is used, as an alternative to the 180° echo generating pulse, to avoid inverting the steady state longitudinal magnetization that is still present when successive signals are observed. Instead of applying a gradient equal to the "read" gradient before the 180° reversing pulse, as in standard spin echo imaging, an equal and opposite gradient is applied, without the 180° pulse. Gradient echos may be used with any TR and TE values.

A number of abbreviations are used for fast sequences using gradient echoes: FLASH (fast low angle shot), FISP (fast imaging steady state precessing), PFI (partial flip imaging), GRASS (gradient refocused acquisition in steady state), and PS (partial saturation). They differ in the methods used to protect against artifacts related to very short TRs. These artifacts occur if coherent transverse magnetization remains when the next excitation pulse is applied. To eliminate this artifact, special gradients are applied after each data acquisition, either to spoil the coherence of the residual magnetization or to make it uniform from one repetition to the next.

The importance of these sequences to hematoma imaging is that they are sensitive to field inhomogeneity, i.e., to $T2^*$. This sensitivity can be increased by using longer TEs. T1 sensitivity can be reduced by using small flip angles, e.g., 10 or 15° (41).

II. Evolution of Hematomas

We will now see how the three relaxation mechanisms shown in Table 1 and proton density contribute to image contrast during the various stages of hematoma evolution. This discussion is necessarily oversimplified. Though the five stages described below (see Fig. 2) are typical of many hematomas, the timing of the phases may vary significantly and, of course, different phases may overlap. In fact, we have opted not to correlate these phases with the clinical stages (hyperacute, acute, subacute, subchronic, chronic) or with definite time periods. As in other areas of diagnostic imaging, variability is
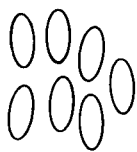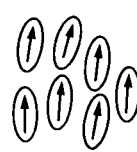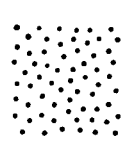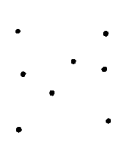
OXY	DEOXY	MET	HEMOLYSIS	RESORPTION
High field	High field			
o T2* WI	o T2 & T2* WI	High and Med fields	High and Med fields	
		● T1 WI	● T1 WI	All fields
Med field	Med field	o T2 & T2* WI	● T2 WI	o T1 WI
● STIR (?)	o T2* WI			● T2WI
Low field	Low field	Low field	Low field	
● T1 WI	● T1 WI	● T1 WI	● T1 WI	
		o T2 WI (?)		

FIG. 2. Image contrast at five hematoma stages. Illustrations schematically depict each stage, with arrows indicating paramagnetic forms of hemoglobin. The imaging sequences listed are those known or believed to yield strong and reliable contrast in the indicated field range (defined in text). ●, hyperintense to white matter; WI, weighted image; O, hypointense; (?), theoretical.

here the rule and fixed "formulas" will soon prove disappointing. The principal stages are illustrated by clinical images taken at either 0.25 or 1.5 T (Figs. 3–9).

Another caveat has to do with overinterpreting the theory. Though the mechanisms described earlier have a sound theoretical and experimental basis, they are not completely understood in complex biological tissue, and they probably do not tell the whole story. For example, we may state confidently that inhomogeneous susceptibility causes hypointensity on T2-weighted images, but we cannot state precisely how much.

Before discussing the hematoma proper, we must mention the frequent appearance of edema. Both acute and chronic hematomas are often surrounded by a complete or partial ring of edema with elevated T1 and T2 related to high fluid content and low protein concentration. Though the MR appearance of blood is variable, the edema is constant and unmistakable: dark on T1-weighted images and bright on T2-weighted or STIR images. Surrounding edema can be helpful in delineating the lesion, but must not be confused with the actual blood.

A. Oxygenated Blood

Whether the hemorrhage is arterial or venous, a fresh bleed is usually fairly well oxygenated. Therefore, image appearance is determined primarily by protein effects and proton density.

Image appearance. T1 and T2 in oxygenated whole blood are both longer than in cerebral white matter (16,42). Though we would expect the longer T1 to lead to hypointensity on T1-weighted images, this effect is counteracted by the higher proton density and higher T2 of whole blood, and shortening of T1 with clot retraction may further contribute to hyperintensity. The result, at medium and high fields, is an image intensity not much different from the white-gray matter range (12,13,16,37,43,44), as
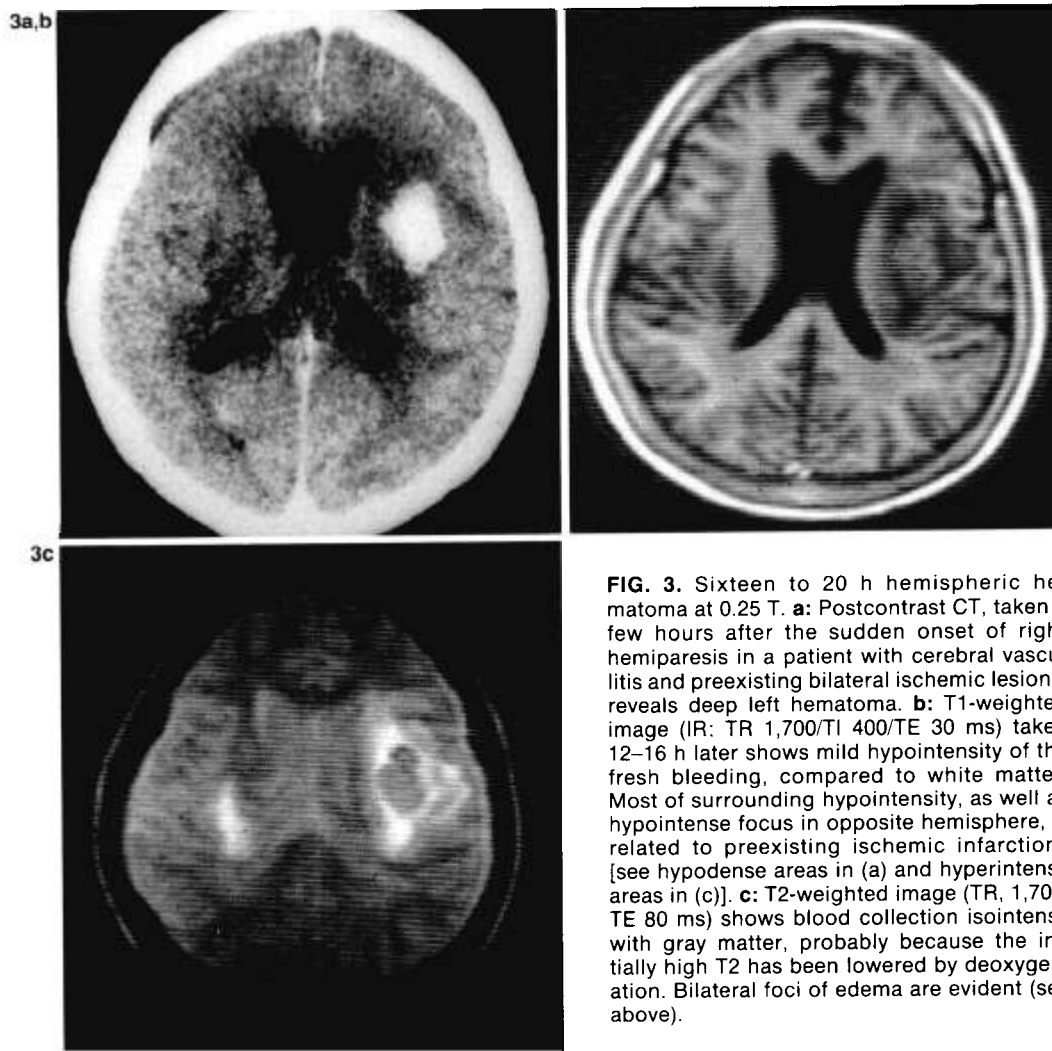

FIG. 3. Sixteen to 20 h hemispheric hematoma at 0.25 T. **a:** Postcontrast CT, taken a few hours after the sudden onset of right hemiparesis in a patient with cerebral vasculitis and preexisting bilateral ischemic lesions, reveals deep left hematoma. **b:** T1-weighted image (IR: TR 1,700/TI 400/TE 30 ms) taken 12–16 h later shows mild hypointensity of the fresh bleeding, compared to white matter. Most of surrounding hypointensity, as well as hypointense focus in opposite hemisphere, is related to preexisting ischemic infarctions [see hypodense areas in (a) and hyperintense areas in (c)]. **c:** T2-weighted image (TR, 1,700/TE 80 ms) shows blood collection isointense with gray matter, probably because the initially high T2 has been lowered by deoxygenation. Bilateral foci of edema are evident (see above).

FIG. 4. One day hemispheric hematoma at 1.5 T. **a:** One day after clinical deterioration in a patient with known preexisting left infarction, a T1-weighted image (TR 500/TE 15 ms) shows slightly hyperintense discrete central focus (arrow). **b:** On T2-weighted image (TR 2,000/TE 90 ms), blood is hypointense (arrow) because of the inhomogeneous susceptibility created by intracellular deoxyhemoglobin.
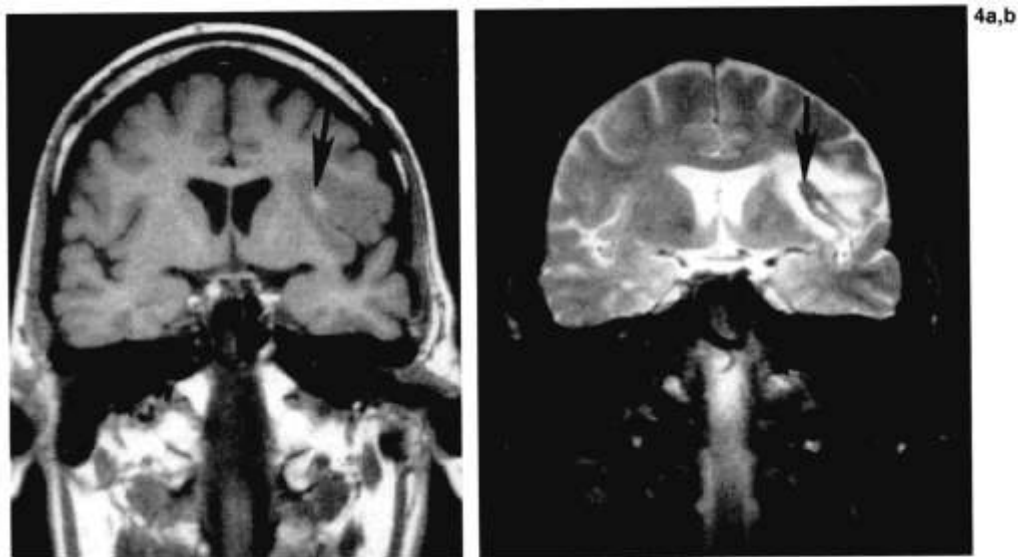
illustrated in Figs. 3b and 4a. It is worth noting that a STIR sequence might offer better contrast because the initially longer T1 would then combine with higher proton density to produce hyperintensity. At low fields the picture is different, with a marked hyperintensity on T1-weighted images reported (18). This may be related to a relatively stronger protein effect at low fields (see Theory).

Very early T2-weighted images of oxygenated hematomas show hyperintensity (16,37) because of both the longer T2 and the increased proton density, but the brightness disappears quickly with deoxygenation (Fig. 3c), especially at high fields, and, due to its extremely transient nature, cannot be relied on for clinical diagnosis.

B. Deoxygenation

Deoxygenation begins immediately and is probably complete by 24 h in the absence of rebleeding or oxygen supply (45). The resulting inhomogeneous susceptibility, due to paramagnetic deoxyHb within the red blood cells, reduces the effective T2 at high and, to a lesser extent, medium fields. The reduction in T2* is even greater, but T1 is not affected. However, a simultaneous increase in hematocrit may occur due to clot retraction, and this reduces T1 at low fields and furthur reduces T2 at all fields.

Image appearance. The inhomogeneous susceptibility causes a marked hypointensity on T2-weighted images of hematomas at high fields (Figs. 4b, 5c, and 6b), as was first pointed out by DeLaPaz et al. (13) and Gomori et al. (14). Gomori et al. also noted that the hypointensity occurs earliest in the center of the hematoma, consistent with the more limited oxygen supply to that area. T2-weighted hypointensity has also been seen at 0.5 T (16,37,44, 46). However, some (or most) of the observed hy-

pointensity (depending on field strength) may be due to clot retraction (28), since a high hematocrit increases the protein effect and reduces the inhomogeneous susceptibility effect. The hypointensity is stronger on T2*-weighted (gradient echo) sequences (Fig. 6c), even at medium fields (17,42,43). In fact, at high fields the hypointensity appears so early as to suggest that there might be some mechanism, other than deoxyHb, responsible (47). A pitfall of gradient echo images is that artifactual hypointensity near air cavities may mimic or obscure hematomas (48,49), while intralesional signal characteristics may be obscured by the strong hypointensity (50).

T1-weighted images are not affected by deoxygenation (Fig. 4a), although, at low fields, clot retraction may add to the already existing hyperintensity.

C. Methemoglobin Conversion

The time scale for the conversion of deoxyHb to metHb in a hematoma is several days. An in vitro study (51) showed that intracellular metHb in whole blood at 37°C begins to accumulate at a rate of 10–12%/day after the first 2 days. Adams and Sidman (52) state that in aneurysmal hemorrhage, metHb begins to appear after a few hours; petechial hemorrhages after several weeks or more often appear chocolate brown, indicating the presence of metHb. Methemoglobin causes a reduction in both T1 and T2 at all fields.

Image appearance. The T1 reduction creates hyperintensity on T1-weighted images (15), becoming noticeable at ~3 or 4 days (12,16,37). (At low fields this merely reinforces the preexisting hyperintensity.) The metHb effect often appears first at the periphery (Fig. 5b) and later throughout the he-
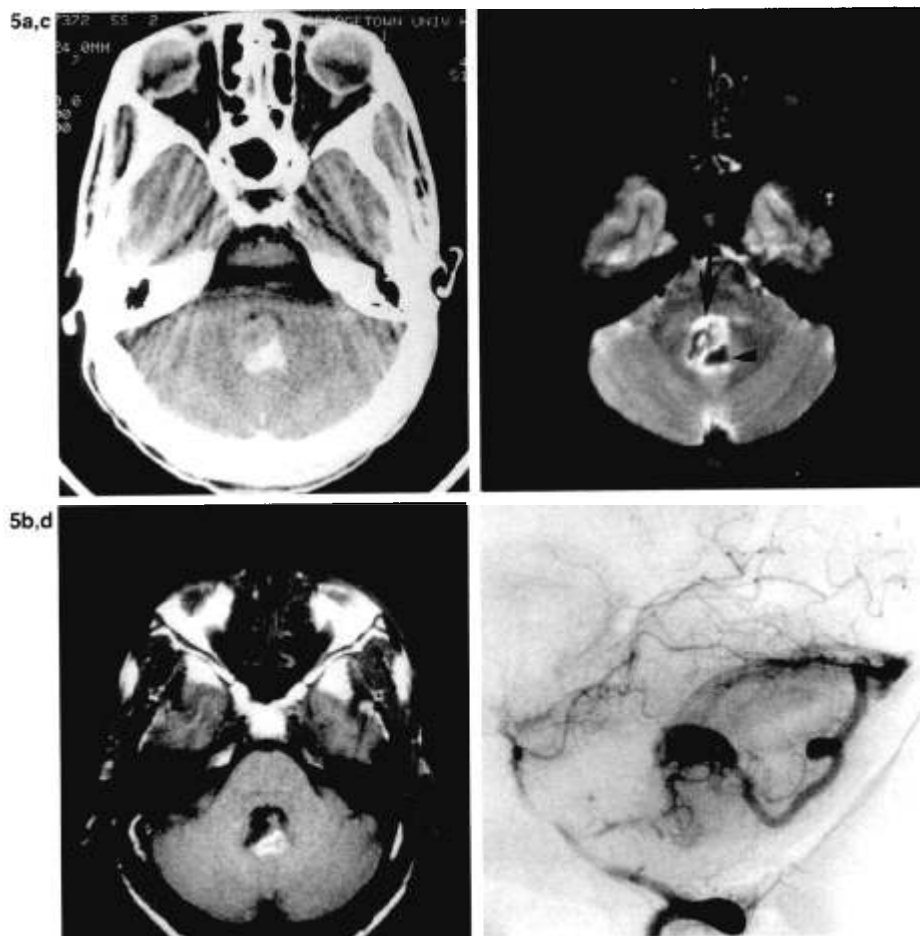
FIG. 5. Four day posterior fossa hematoma at 1.5 T. **a:** Posterior fossa noncontrast CT scan 2 days after sudden onset of symptomatology consistent with intracranial bleeding in a patient with arteriovenous malformation (AVM) close to fourth ventricle. Blood collection at site is obvious. **b:** Two days later, T1-weighted image (TR 600/TE 15 ms) shows isointense (to cerebellum) centrum with peripheral hyperintensity as methemoglobin begins to form. Markedly hypointense areas anterior to extravasated blood are AVM vessels (flow). **c:** T2-weighted image (TR 2,500/TE 80 ms) shows marked hypointensity in center of hematoma (arrowhead) as deoxygenation is probably complete. Irregularly distributed edema and compressed slit-like fourth ventricle (arrow, also see CT) appear as hyperintense areas. Note also flow void effect in adjacent AVM vessels. **d:** Arteriogram.

matoma (Figs. 6a, 7b, and 8a) (16,44). Similarly, the T2 reduction reinforces the preexisting hypointensity seen on T2- or T2*-weighted images at medium and high fields, and hence does not change the image appearance.

D. Hemolysis

Hemolysis refers to the escape of Hb from the red blood cells by fragmentation and osmotic lysis (53). We have not been able to find pathological data as to when this occurs in hematomas. Hemolysis eliminates the inhomogeneous susceptibility effect and reduces the protein effect as the Hb becomes uniformly distributed. Thus, we expect to see longer T2s and also longer T1s at low fields.

Image appearance. A reappearance of hyperintensity on T2-weighted images (Figs. 7c and 8b), beginning at ~1 week, has been noted and linked to

hemolysis (13,14,44). We refer to this as "rebound hyperintensity." On the other hand, T1-weighted images are not affected by hemolysis at medium and high fields, and hence continue to show hyperintensity (Figs. 7b and 8a). This paradoxical state of long T2 and short T1 may continue for 1 month or more (13). However, the linkage of the "rebound" T2-weighted hyperintensity with hemolysis has not been proven, and there are clearly other changes, such as protein resorption, which may also contribute to the image appearance and its continuation over a fairly long time.

E. Protein Resorption and Hemosiderin

Following the breakdown of red blood cells, there is an osmotically induced influx of cerebrospinal fluid, which dilutes the protein concentration (5), and a gradual removal of Hb from the central he-
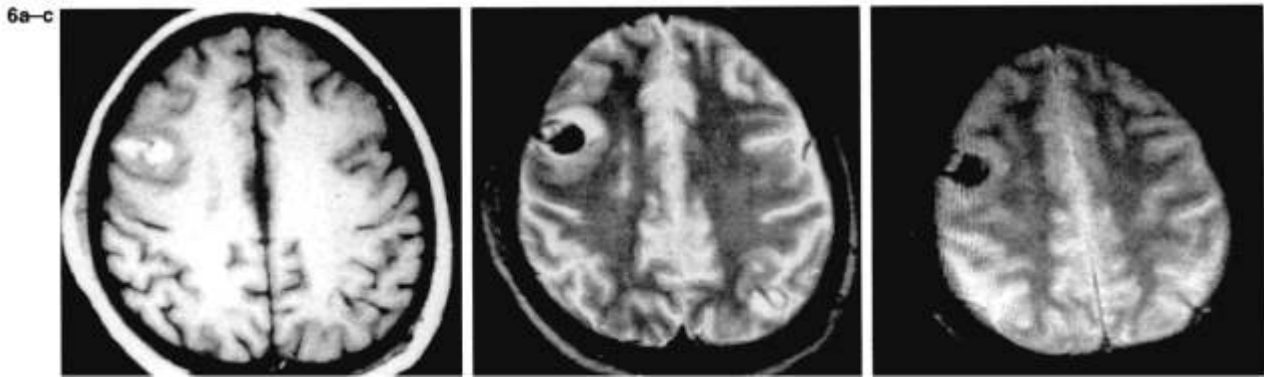
6a—c

FIG. 6. Four and one-half day superficial hematoma (related to traumatic shunt removal) at 1.5 T. Surrounding edema is present in all images. **a:** In T1-weighted image (TR 600/TE 15 ms), blood is hyperintense because of enhanced relaxation caused by paramagnetic methemoglobin (metHb). **b:** In T2-weighted image (TE 2,500/TE 80 ms), blood is hypointense owing to combination of inhomogeneous susceptibility and paramagnetic relaxation with metHb. **c:** In T2*-weighted image (FISP, TR 200/TE 10 ms, flip angle = 10°), blood also shows strong hypointensity because of inhomogeneous susceptibility effect.

matoma by phagocytosis (52). The CT evidence indicates that this occurs after 2–6 weeks (1–5). The removal of protein reduces and eventually eliminates the remaining protein and paramagnetic relaxation mechanisms. That is, as the lesion approaches a cyst-like state, the fraction of water close to large molecules and paramagnetic particles becomes very small, and T1 and T2 ultimately approach those of cerebrospinal fluid. An increase in proton density also accompanies this process. On the other hand, the deposition of iron-laden hemosiderin in surrounding areas affects the image appearance at those points (14). A recent study has shown that the distribution of ferritin is more extensive than that of hemosiderin, and correlates better with the affected image intensity (54).

Image appearance. As the relaxation times elon-

gate, the appearance on T1-weighted images changes from hyperintense (metHb effect) to hypointense, and T2-weighted images become very hyperintense (Fig. 9c) at all fields. The Hb removed from the body of the lesion is converted into hemosiderin and ferritin and tends to accumulate at the border of the hematoma. This accumulation causes a low effective T2 and T2* because of the inhomogeneous susceptibility effect, and hence shows up as a dark rim on T2- or T2*-weighted images at medium and high fields (Figs. 8b and 9c). In later (1 to several years after onset) images of the hematoma, it is not infrequent in T2- or T2*-weighted images to note a garland of hyperintensity surrounding the hemosiderin rim (Fig. 9c). This is due to gliosis and should not, of course, be confused with the earlier occurrence of edema.
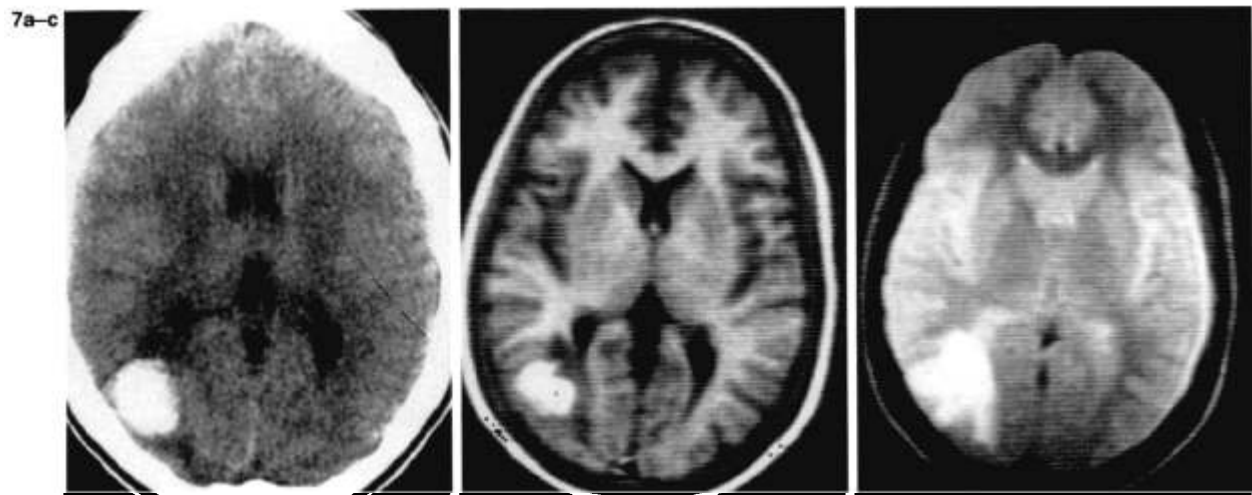
7a—c

FIG. 7. One week hematoma at 0.25 T. **a:** Twenty-four hours after sudden onset of seizures, noncontrast CT shows right posterior bleeding. **b:** T1-weighted image (IR: TR 1,700/TI 400 ms) 5 days later shows hyperintense right blood collection (T1 lowering by methemoglobin) easily separated from hypointense edema. **c:** T2-weighted image (TR 1,700/TE 80 ms) shows hyperintensity because hemolysis has eliminated the susceptibility effect and reduced the protein effect on T2.
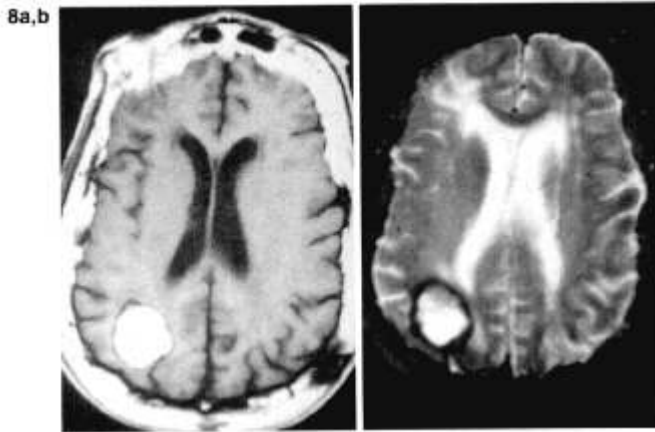
FIG. 8. Three week right posterior hemispheric hematoma at 1.5 T. **a**: T1-weighted image (TR 600/TE 15 ms) shows hyperintensity due to continued presence of methemoglobin. **b**: T2-weighted image (TR 2,500/TE 80 ms) is hyperintense as in Fig. 5c. Thin surrounding dark band is due to hemosiderin/ferritin laden macrophages. A slight dark band from hemosiderin/ferritin can also be seen in (a). Right frontal lobe changes are of ischemic nature.

F. Other Effects

The above material presents the principal hematoma stages that have been reported to occur in most intraparenchymal hematomas. We now mention several other factors that either have not been studied enough, or do not occur consistently enough, to warrant inclusion in the "standard" sequence.

Clot formation. Clotting often occurs in the early stage of a hematoma, but there is not much indication that fibrin strands per se affect the MR parameters. Clotted and unclotted blood was compared at

0.15 T by Cohen et al. (55), who found no difference in T1. Though Rapoport et al. (56) reported that T1 and T2 were shorter in clotted than in unclotted blood, their anomalously high values for unclotted blood (T1 1,300 ms, T2 320 ms at 0.5 T) suggest an artifactual explanation, such as changes in hematocrit.

Hematoma size and location. The presence and timing of the above effects, or stages, may well depend on hematoma size and location. For example, Gomori and Grossman (57) reported that hemorrhagic cortical infarctions show less deoxygenation effect and are more diffuse, frequently petechial, without a clear separation of hemosiderin deposits. Fobben et al. (58) found little hemosiderin accumulation around subdural hemorrhages, which they attribute to removal of macrophages by the bloodstream. It has been pointed out (59) that T1 contrast, although minimal in most hematomas, may be useful for identifying subarachnoid hemorrhage in normal cerebrospinal fluid cavities.

Rebleeding. The occurrence of rebleeding, i.e., the introduction of fresh arterial blood into the hematoma, even weeks or months after ictus, is a not uncommon complication (37). The simultaneous presence of various stages of hematoma evolution can make interpretation extremely difficult.

SUMMARY

Once the radiologist has wrestled with and solved the complex problems of image interpretation, the greatest challenge to the diagnosis of hematomas with MR is probably in the very early hyperacute phase, when the blood is well oxygenated and contrast mechanisms are not strong or reliable. Com-
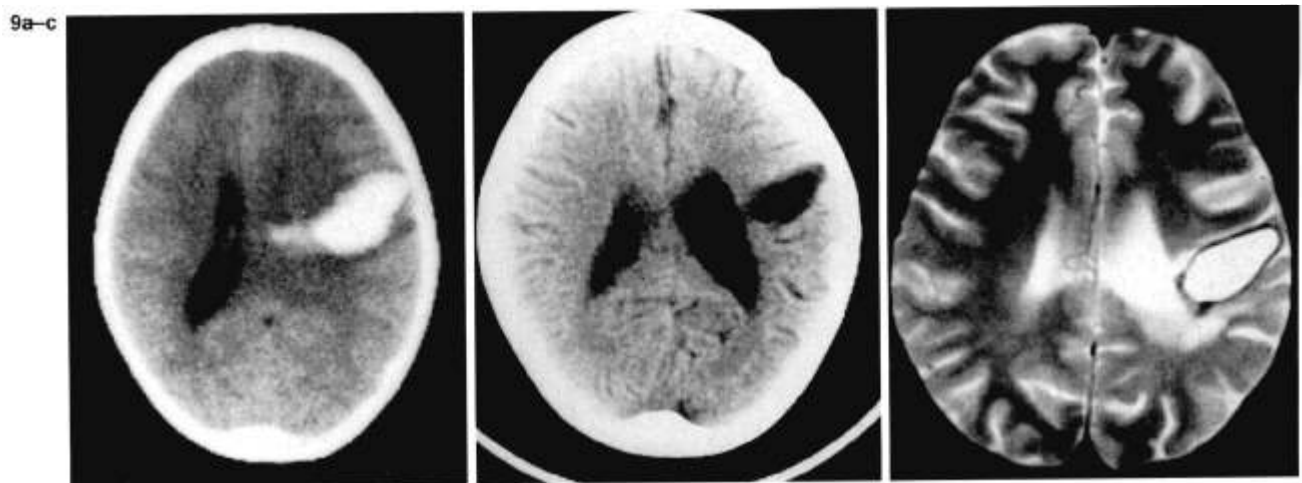

FIG. 9. Four year sequela of hemispheric hematoma at 1.5 T. In 1984 CT (**a**) shows left hematoma, the sequela of which, 4 years later (**b**), is evident as a porencephalic cavity. At this time (**c**) T2-weighted image (TR 2,500/TE 80) shows fluid filled cavity with hypointense hemosiderin/ferritin rim and peripheral hyperintensity (gliosis). T1-weighted image (not available) would similarly show hypointensity characteristic of fluid.

puted tomography may still be considered the most reliable method, although small lesions may not be noticed with CT. Low field MR affords good detection because of T1 contrast, but very few such scanners are in use today. For the vast majority of scanners, T2*-weighted gradient echo sequences offer the best early detectability, whereas T2-weighted images are effective as deoxygenation proceeds, particularly at the highest fields. A short T1 sequence with short TE (STIR) may also provide good early hematoma contrast because of the reinforcing effect of high proton density and long T1.

After sufficient deoxygenation has occurred (usually within 24 h, depending on field strength), detection at medium and high fields becomes more reliable because of the striking hypointensity on T2-weighted images. At this stage, the T1-weighted image serves as a useful time indicator of the hematoma by indicating the formation of metHb.

Still later, T2–T2* hypointensity disappears, probably due to hemolysis, and is replaced with "rebound" hyperintensity, while continued T1-weighted brightness shows the continuing presence of metHb. In the final stages, the long range hallmarks of cystic formation and (at medium and high fields) hemosiderin/ferritin accumulation are unmistakable.

NOTE ADDED IN PROOF:

The references to Zhong et al. (unpublished data) should be replaced by: Zhong J, Gore JC, Armitage IM. Quantitative studies of hydrodynamic effects and cross relaxation in protein solutions and tissues with proton and deuteron longitudinal relaxation times. *Magn Reson Med*, 1989. In press. Zhong J, Gore JC, Armitage IM. Relative contributions of chemical exchange and other relaxation mechanisms in protein solutions and tissues. *Magn Reson Med*, 1989. In press.

REFERENCES

1. Scott WR, New PFJ, Davis KR, Schnur JA. Computerized axial tomography of intracerebral and intraventricular hemorrhage. *Radiology* 1974;112:73–80.
2. New PFJ, Aronow S. Attenuation measurements of whole blood and blood fractions in computed tomography. *Radiology* 1976;121:635–40.
3. Norman D, Price D, Boyd D, Fishman R, Newton TH. Quantitative aspects of computed tomography of the blood and cerebrospinal fluid. *Radiology* 1977;123:335–8.
4. Forbes GS, Sheedy PF, Piepgras DG, Houser OW. Computed tomography in the evaluation of subdural hematomas. *Radiology* 1978;126:143–8.
5. Brihaye J. Chronic subdural hematoma. In: McLaurin RL, ed. *Extracerebral collections.* New York: Springer-Verlag, 1986:101–56.
6. Bydder GM, Steiner RE, Young IR, et al. Clinical NMR imaging of the brain: 140 cases. *AJNR* 1982;3:459–80.
7. Crooks LE, Mills CM, Davis PL, et al. Visualization of cerebral and vascular abnormalities by NMR imaging. The effects of imaging parameters on contrast. *Radiology* 1982;144:843–52.
8. Brant-Zawadzki M, Davis PL, Crooks LE, et al. NMR demonstration of cerebral abnormalities: comparison with CT. *AJNR* 1983;4:117–24.
9. Crooks LE, Ortendahl DA, Kaufman L, et al. Clinical efficiency of nuclear magnetic resonance imaging. *Radiology* 1983;146:123–8.
10. Moon KL Jr, Brant-Zawadzki M, Pitts LH, Mills CM. Nuclear magnetic resonance imaging of CT-isodense subdural hematomas. *AJNR* 1984;5:319–22.
11. Herfkens R, Davis PL, Crooks LE, et al. Nuclear magnetic resonance imaging of the abnormal live rat and correlations with tissue characteristics. *Radiology* 1981;141:211–8.
12. Sipponen JT, Sepponen RE, Sivula A. Nuclear magnetic resonance (NMR) imaging of intracerebral hemorrhage in the acute and resolving phases. *J Comput Assist Tomogr* 1983;7:954–9.
13. DeLaPaz RL, New PFJ, Buonanno FS, et al. NMR imaging of intracranial hemorrhage. *J Comput Assist Tomogr* 1984;8:599–607.
14. Gomori JM, Grossman RI, Goldberg HI, Zimmerman RA, Bilaniuk LT. Intracranial hematomas: imaging by high-field MR. *Radiology* 1985;157:87–93.
15. Bradley WG Jr, Schmidt PG. Effect of methemoglobin formation on the MR appearance of subarachnoid hemorrhage. *Radiology* 1985;156:99–103.
16. Di Chiro G, Brooks RA, Girton ME, et al. Sequential MR studies of intracerebral hematomas in monkeys. *AJNR* 1986;7:193–9.
17. Edelman RR, Johnson K, Buxton R, et al. MR of hemorrhage: a new approach. *AJNR* 1986;7:751–6.
18. Sipponen JT, Sepponen RE, Tanttu JI, Sivula A. Intracranial hematomas studied by MR imaging at 0.17 and 0.02 T. *J Comput Assist Tomogr* 1985;9:698–704.
19. Brooks RA, Di Chiro G. Magnetic resonance imaging of stationary blood: a review. *Med Phys* 1987;14:903–13.
20. Bloembergen N, Purcell EM, Pound RV. Relaxation effects in nuclear magnetic resonance absorption. *Phys Rev* 1948;73:679.
21. Bloembergen N. *Nuclear magnetic relaxation.* (This reprint volume contains Bloembergen's Ph.D. thesis.) New York: Benjamin 1961:81–6.
22. Simpson JH, Carr HY. Diffusion and nuclear spin relaxation in water. *Phys Rev* 1958;111:1201.
23. Meiboom S. Nuclear magnetic resonance study of the proton transfer in water. *J Chem Phys* 1961;34:375–88.
24. Koenig SH. The dynamics of water-protein interactions. In: Rowland SP, ed. *Water in polymers.* Washington, DC: American Chemical Society, 1980:157–76. (ACS Symposium Series; no 127).
25. Lindstrom TR, Koenig SH. Magnetic-field-dependent water proton spin-lattice relaxation rates of hemoglobin solutions and whole blood. *J Magn Reson* 1974;15:344–53.
26. Lindstrom TR, Koenig SH, Boussios T, Bertles JF. Intermolecular interactions of oxygenated sickle hemoglobin molecules in cells and cell-free solutions. *Biophys J* 1976;16:679–89.
27. Gomori JM, Grossman RI, Yu-lp C, Asakura T. NMR relaxation times of blood: dependence on field strength, oxidation state, and cell integrity. *J Comput Assist Tomogr* 1987;11:684–90.
28. Hayman LA, Ford JJ, Taber KH, Saleem A, Round ME, Bryan RN. T2 effect of hemoglobin concentration: assessment with in vitro MR spectroscopy. *Radiology* 1988;16:489–91.
29. Brindle KM, Brown FF, Campbell ID, Grathwohl C, Kuchel PW. Application of spin-echo nuclear magnetic resonance to whole-cell systems. *Biochem J* 1979;180:37–44.
30. Brooks RA, Brunetti A, Alger J. On the origin of paramag-

netic inhomogeneity effects in blood. *Magn Reson Med* 1989 (in press).

31. Thulborn KR, Waterton JC, Matthews PM, Radda GK. Oxygenation dependence of the transverse relaxation time of water protons in whole blood at high field. *Biochim Biophys Acta* 1982;714:265–270.

32. Meiboom S, Gill D. Modified spin-echo method for measurements of relaxation times. *Rev Sci Instrum* 1958;29:688.

33. Gillis P, Koenig SH. Transverse relaxation of solvent protons induced by magnetized spheres: application to ferritin, erythrocytes, and magnetite. *Magn Reson Med* 1987;5:323–45.

34. Koenig SH, Brown RD III, Lindstrom TR. Interactions of solvent with the heme region of methemoglobin and fluoromethemoglobin. *Biophys J* 1981;34:397.

35. Dittmer DS, ed. *Blood and other body fluids.* Washington, DC: Federation of American Societies for Experimental Biology, 1961:19.

36. Suzuki K. Chemistry and metabolism of brain lipids. In: Siegel GJ, Albers RW, Agranoff BW, Katzman R, eds. *Basic neurochemistry.* 3rd ed. Boston: Little, Brown, 1981:355.

37. Zimmerman RD, Heier LA, Snow RB, Liu DPC, Kelly AB, Deck MDF. Acute intracranial hemorrhage: intensity changes on sequential MR scans at 0.5 T. *AJNR* 1988;9:47–57.

38. Hackney DB, Atlas SW, Grossman RI, et al. Subacute intracranial hemorrhage: contribution of spin density to appearance on spin-echo MR images. *Radiology* 1987;165:199–202.

39. Bydder GM, Young IR. MR imaging: clinical use of the inversion recovery sequence. *J Comput Assist Tomogr* 1985; 9:659–75.

40. Frahm J, Haase A, Matthaei D. Rapid NMR imaging of dynamic processes using the FLASH technique. *Magn Reson Med* 1986;3:321–7.

41. Buxton RB, Edelman RR, Rosen BR, Wismer GL, Brady TJ. Contrast in rapid MR imaging: T1- and T2-weighted imaging. *J Comput Assist Tomogr* 1987;11:7–16.

42. Bottomley PA, Foster TH, Argersinger RE, Pfeifer LM. A review of normal tissue hydrogen NMR relaxation times and relaxation mechanisms from 1–100 MHz: dependence on tissue type, NMR frequency, temperature, species, excision, and age. *Med Phys* 1984;11:425–48.

43. Nose T, Enomoto T, Hyodo A, et al. Intracerebral hematoma developed during MR examination. *J Comput Assist Tomogr* 1987;11:184–7.

44. Komiyama M, Baba M, Hakuba A, Nishimura S, Inoue Y. MR imaging of brainstem hemorrhage. *AJNR* 1988;9:261–8.

45. Altman PL, Gibson JF Jr, Wang CC. *Handbook of respiration.* Philadelphia: WB Saunders, 1958.

46. Zimmerman RD, Deck MDF. Intracranial hematomas: imaging by high-field MR. *Radiology* 1986;159:565.

47. Weingarten K, Zimmerman RD, Markisz J, Cahill P, Sze G, Deck MDF. The effect of hemoglobin oxygenation on the MR intensity of experimentally produced intracerebral hematomas at 0.6 and 1.5 T. Annual Meeting of the American Society of Neuroradiology, Chicago, May 15–20, 1988.

48. Bydder GM, Payne JA, Collins AG, et al. Clinical use of rapid T2 weighted partial saturation sequences in MR imaging. *J Comput Assist Tomogr* 1987;11:17–23.

49. Winkler ML, Olsen WL, Mills TC, Kaufman L. Hemorrhagic and nonhemorrhagic brain lesion: evaluation with 0.35 T fast MR imaging. *Radiology* 1987;165:203–7.

50. Atlas SW, Mark AS, Grossman RI, Gomori JM. Intracranial hemorrhage: gradient-echo MR imaging at 1.5 T. *Radiology* 1988;168:803–807.

51. Jandl JH, Engle LK, Allen DW. Oxidative hemolysis and precipitation of Hb. I. Heinz body anemias as an acceleration of red cell aging. *J Clin Invest* 1960;39:1818–36.

52. Adams RD, Sidman RL. *Introduction to neuropathology.* New York: McGraw-Hill, 1968.

53. Wintrobe MM. *Clinical hematology.* Philadelphia: Lea & Febiger, 1974.

54. Thulborn KR, McKee A, Kowall NW, Moore J, Richardson EP, Rosen BR, Brady TJ. Magnetic suspectibility of ferritin as the primary determinant of the appearance of late phase cerebral hematoma on T2 weighted magnetic resonance images. 7th Ann Meeting Soc Magn Reson Med, San Francisco, August 1988, p. 583.

55. Cohen MD, McGuire W, Cory DA, Smith JA. MR appearance of blood and blood products: an in vitro study. *AJR* 1986;146:1293–7.

56. Rapoport S, Sostman HD, Pope C, Camputaro CM, Holcomb W, Gore JC. Venous clots: evaluation with MR imaging. *Radiology* 1987;162:527–30.

57. Gomori JM, Grossman RI. Head and neck hemorrhage. In: Kressel HY, ed. *Magnetic resonance annual 1987.* New York: Raven Press, 1987:71–112.

58. Fobben ES, Grossman RI, Hackney DB, Goldberg HI, Zimmerman RA, Bilaniuk LT. The MRI appearance of subdural hematomas and hygromas at 1.5 Tesla. Annual Meeting of the American Society of Neuroradiology, Chicago, May 15, 1988.

59. Yoon HC, Lufkin RB, Vinuela F, Bentson J, Martin N, Wilson G. MR of acute subarachnoid hemorrhage. *AJNR* 1988;9:404–5.